BULLETIN OF THE POLISH ACADEMY OF SCIENCES
TECHNICAL SCIENCES, Vol. 68, No. 1, 2020
DOI: 10.24425/bpasts.2020.131832

Application of acoustic emission to monitoring the course of the alkali-silica reaction

G. ŚWIT and J. ZAPAŁA-SŁAWETA*

Kielce University of Technology

Abstract. The study presented research on the possibility of using acoustic emission to detect and analyze the development of the alkali-silica reaction (ASR) in cement mortars. The experiment was conducted under laboratory conditions using mortars with reactive opal aggregate, accelerating the reaction by ensuring high humidity and temperature, in accordance with ASTM C227. The progress of corrosion processes was monitored continuously for 14 days. The tests were complemented with measurements of the expansion of the mortars and observations of microstructures under a scanning electron microscope. The high sensitivity of the acoustic emission method applied to material fracture caused by ASR enabled the detection of corrosion processes already on the first day of the test, much sooner than the first recorded changes in linear elongation of the specimens. Characteristic signal descriptors were analyzed to determine the progress of corrosion processes and indicate the source of the cracks. Analysis of recorded 13 AE parameters (counts total, counts to peak, duration, rise time, energy, signal strength, amplitude, RMS, ASL, relative energy, average frequency, initial frequency and reverberation frequency) indicates that the number of counts, signal strength and average frequency provide most information about the deleterious processes that occur in the reactive aggregate mortars. The values of RA (rise time/amplitude) and AF (average frequency) enabled the classification of detected signals as indicating tensile or shear cracks. The acoustic emission method was found suitable for monitoring the course of alkali-aggregate reaction effects.

Key words: alkali-silica reaction, acoustic emission, corrosion, microstructure, AE descriptors.

1. Introduction

Corrosion processes resulting from physical factors, so-called freeze-thaw cycles, shrinkage, erosion and salt crystallization, and chemical factors, i.e. sulphate corrosion, acid corrosion, alkali-aggregate reaction and biological corrosion, are all causes of insufficient concrete durability [1]. The cracks caused by product swelling or weakening of the structure due to the dissolution/leaching of hydration products result in the deterioration of the mechanical properties of the material [2–4]. Alkali-silica reaction (ASR) was a cause of damage to concrete structures that was particularly frequent in the United States, in structures erected from the 1920s to 1940s. Since then, aggregate reactivity has become a subject of intensive scientific research [5–9]. In Poland, no reduction of durability of actual concrete structures due to the ASR has been observed so far; however, the presence of aggregate demonstrating alkali reactivity was confirmed in certain regions of Poland [10–13]. The alkali-aggregate reaction is a heterogeneous reaction of reactive forms of amorphous or poorly crystalline silica with sodium and potassium hydroxides dissolved in the solution in concrete pores [14]. The process takes place in two stages: during the first stage, acidic silanol groups react with sodium and potassium hydroxides, leading to the formation of alkali silica and silicic acid, which then reacts with hydroxyl ions, creating additional portions of an amorphous and strongly hygroscopic gel. During the second stage, the products swell up osmotically due to water absorption [15, 16]. The reaction results in the formation of products of volume distinctly greater than the original volume of silica aggregate. The degree of swelling of gel products depends on the density of the gel created and on the amount of water absorbed. Swelling sodium-potassium-calcium silica gel causes cracking of the aggregate and surrounding cement paste [17]. Depending on the degree of reactivity of the aggregate and on the reaction mechanism, corrosion products may also accumulate in air pores [18, 19].

The methods for assessing the degree of concrete degradation due to ASR usually involve visual inspection and tests of collected concrete cores. A mesh of cracks or gel exudations may be observed on the concrete surface and may be misinterpreted as results of frost corrosion or leaching corrosion. This is largely dependent on the experience of the inspector [20]. Determination of the advancement of corrosion processes, frequently based on compressive strength tests of concrete, is not particularly effective, either, because ASR only exerts a small adverse impact on this strength [2]. Also, there are other active corrosion processes that may have an adverse effect on strength [21]. Among the many methods for detection of internal corrosion, non-destructive methods are of particular importance [20]. The most frequently used method is the ultrasonic concrete test (UPV test), which measures the velocity of ultrasonic waves passing through the material. Any cracks or discontinuities of the material affect attenuation, time of wave propagation and formation of the waves being reflected. There exist many analyses indicating that the UPV method enables the detection of primarily surface cracks caused by ASR [22]. Recorded changes of wave propagation velocity were small even at significant specimen expansion levels [23].

*e-mail: jzapala@tu.kielce.pl

Manuscript submitted 2019-02-13, revised 2019-08-26, initially accepted for publication 2019-11-04, published in February 2020

Correct identification of alkali corrosion requires methods that enable monitoring of the affected structure and determination of the location of cracks [24, 25]. Such capabilities are provided by the acoustic emission method (AE) [24–26]. It is a non-invasive, passive, non-destructive method commonly used in the examination of concrete exposed to corrosion [27–29]. AE equipment records physical effects that occur spontaneously in the tested material, i.e. the equipment does not emit any signals and, therefore, does not affect the physical condition of the tested facility [30]. Corrosion processes in concrete reduce internal energy, becoming a source of an AE signal. High-frequency ultrasonic waves propagate in all directions in the material. The acoustic emission wave reaches the sensor and then the AE analyzer in the form of voltage variations. The AE signal is characterized by a number of parameters that provide information about the AE source [30–32]. Acoustic waves are generated by so-called active damage, i.e. damage forming or developing during the measurement. Therefore, acoustic emission may be used to monitor corrosion processes during which the cracks form or develop. It is a promising method for the testing and monitoring of active corrosion processes, both *in situ* and under laboratory conditions [33, 34].

The emission method was adapted to measurements of alkali corrosion in rock and concrete samples, conducted primarily under laboratory conditions, fairly recently, in the second decade of the 21st century. The tests were conducted on specimens of mortars with reactive aggregate, using the accelerated testing methodology in accordance with ASTM C1260, and concrete specimens in accordance with ASTM C1293 [35–37]. The results of the analyses indicated that AE enabled the detection of early ASR cracking of concrete; at later test stages, particularly with an increased degree of cracking and gel formation, elastic wave attenuation was observed [38].

An analysis of the destructive process in unloaded early-age concrete, concerning mainly concrete shrinkage due to water evaporation, was published in [39]. To assess the processes involved, the acoustic emission method was used based mainly on the energy of AE signals and on modification of this parameter. From observations of other researchers, e.g. Ono et al. and Ohtsu et al. [40, 41], the use of energy of AE signals and the sum of energy are subject to a high degree of uncertainty. This is due to the fact that the values of these parameters, especially the sum of energy, are strongly influenced by the size of the samples, thus they can only provide information about the intensity of the processes, but cannot indicate the process that induces them. The energy parameter can only be an auxiliary parameter.

In the presented work, the parameters used were less dependent on the effect of scale and more significantly dependent on the mechanisms generating them. These parameters were taken from standard recommendations developed by international scientific bodies, including e.g. JCMS-III B5706 and RILEM recommendations [42, 41]. However, this solution also has certain shortcomings, in particular due to entailing some discretion in establishing a separating line between the areas with the dominance of one of the two destructive processes.

Concrete is an anisotropic material, which is why the authors deem the use of energy parameters (signal strength, RMS) based on the signal waveform mathematical analysis the correct approach for analyzing destructive processes. The use of Fourier analyses in the case of composite materials, such as concrete, is encumbered with a great deal of uncertainty. This results from the heterogeneous structure of concrete. The paper includes an analysis of the corrosion processes with the use of sum and point charts of the signal strength, amplitude parameters and summations in the time function. Such an approach allows for evaluating and identifying the processes' intensity. Corrosion processes were tested in cement mortars stored under the conditions specified in ASTM C227. The specimens were continuously monitored for 14 days, i.e. in the period of largest expansion of mortars with opal aggregate. Characteristic parameters of recorded AE signals were analyzed in order to examine the progress of corrosion processes. This was accompanied by simultaneous analysis of the acoustic activity of mortars with non-reactive aggregate, making it possible to detect signals caused by, in particular, maturing and hardening. The tests were complemented with observations of the microstructure of the mortars under a scanning electron microscope.

Preliminary studies on the use of the acoustic emission method for monitoring the effect of lithium nitrate on the alkali-silica reaction have been published in paper [43]. The results of the research presented in this article constitute follow-up of the works conducted, aimed at applying the AE method to assess the reactivity of aggregates and the progress of corrosive processes.

These tests are the first stage in the use of the acoustic emission method for monitoring corrosion processes in mortars and concretes. The AE method is based on traditional single acoustic emission descriptors (amplitude, average frequency, counts, signal strength) and on the RA factor, which is a product of signal rise time and amplitude, on average frequency. Further research will focus on statistical methods and Kohonen neural networks, used for analyzing AE signals generated by processes accompanying phenomena related to aggregate reactivity.

2. Materials and methods

The tests were conducted using CEM I 42.5R Portland cement with the composition as specified in Table 1. Total alkali content was 0.90% Na_2O_e. Opal aggregate from southern Poland was used as the reactive aggregate. The acquired rock fragments were fragmented mechanically to the 0.5–1 mm fraction. The petrographic analysis of the applied aggregate demonstrated that its primary ingredients were opal (65% vol.) and chalcedony (30% vol.); the remaining portion was made up of small amounts of quartz, talc and goethite [44].

The reactivity of opal aggregate was determined by means of testing potential reactivity of the aggregate, in accordance with ASTM C227 [45]. Opal aggregate was used with grain size distribution of 0.5 to 1.0 mm in the quantity of 6% in relation to the mass of standard quartz sand. The remaining portion of the aggregate was made up of non-reactive quartz sand with grain size distribution meeting the requirements of the standard. The mass ratio of all aggregate to cement was 2.25. The water-ce-

Table 1
Chemical composition of cement [% by weight]

Material	SiO_2	Al_2O_3	Fe_2O_3	CaO	MgO	SO_3	K_2O	N_2O	P_2O_5	LOI[(a)]	N.s.p.[(b)]
Cement	19.07	5.43	2.79	62.99	1.66	3.41	0.99	0.25	0.45	2.25	1.00

[(a)] LOI – loss of ignition, [(b)] N.s.p – parts non-soluble in HCl and Na_2CO_3

ment ratio was kept at 0.47. Two series of 25×25×250 mm mortar bars were prepared, 9 specimens in each series. The first series included mortars with opal aggregate, and the second series consisted of reference specimens made of non-reactive aggregate, i.e. quartz sand, which was also used in the first series. 24 h after forming, all specimens were moved into special containers and placed in a climate chamber. The specimens were kept in closed containers at 38±2°C and 100% relative humidity. Three mortar bars were subject to elongation measurements, and three other bars were monitored by means of acoustic emission.

The specimens were kept in the specified conditions for 14 days. Samples for microscopic analysis were taken from the three remaining mortars from each series after 1, 3, 7, and 14 days.

2.1. Expansion measurements. The extension of mortar bars was measured every day for 14 days. Linear changes of the specimens were referred to the baseline measurement, i.e. measurement following the demolding of mortar bars. The extension of the mortars was measured directly after the specimens were removed from the chamber in order to minimize the measuring error due to the cooling of the specimen and in order to ensure optimum correlation of expansion tests with the results obtained using acoustic emission. The specimens were measured using the Graf-Kaufmann apparatus with accuracy of down to one 0.01 mm.

2.2. Acoustic emission. Acoustic activity of the specimens was measured using resonant piezoelectric sensors with a frequency of 55 kHz, characterized by high sensitivity, and a broadband sensor in the 100–1200 kHz range. This was done in order to verify the measurement of generated AE signals. The sensor system was connected to a 24-channel μSAMOS processor. AE sensors were attached to the mortar bar surface in its central part with a tape and connected to the surface of the mortar using silicone sealant [43]. AE signals were recorded continuously, throughout the entire test. Sensor calibration was conducted before the actual measurements by means of reading the parameters of AE signals generated by a reference source. The reference signal was the HSU-NILSEN source – acoustic signal generated by the fracture of 2H graphite lead of a pencil on the surface of the mortar.

The number and arrangement of AE sensors is dependent on mortar quality (damping factor). As for the test results published in works [46, 47], the maximum spacing of 2.6 m is assumed between the sensors in concrete elements, and up to 1.2 m in cracked concrete elements. When the crack location function (min. 2 sensors) is not used, single sensors placed in the center of the specimen (if the maximum radius does not exceed 60 cm) may be used to record the processes in the whole volume of the sample.

2.3. Scanning electron microscopy. Analyses of mortar microstructure were conducted on specimens with a size of 25×25×10 mm, respectively after 1, 3, 7 and 14 days of reaction. 12-mm-thick strips were cut out from the middle part of mortar specimens, and their surface was ground and then polished mechanically on a diamond washer.

The specimens were observed under the FEI COMPANY QUANTA FEG 205 scanning electron microscope. Magnification of 100–30 000× was used. The surface of the specimens was observed in the backscattered electron detection system. The image of the microstructure was obtained using 15 kV.

3. Results

3.1. Mortar expansion. Figure 1 shows the average expansion of mortars without reactive aggregate and mortars made of non-reactive aggregate. It should be noted that mortars made of non-reactive aggregate demonstrate small linear changes, approximately 0.01% throughout the testing period. Mortar bars with reactive aggregate demonstrated large expansion – 0.19% after 14 days. In accordance with ASTM C227, aggregate should be classified as reactive if mortar expansion exceeds 0.05% by the 90th day of reaction and 0.1% after 90 days. In the case being analyzed, mortar bars with the opal aggregate exceeded the aggregate reactivity threshold very quickly.

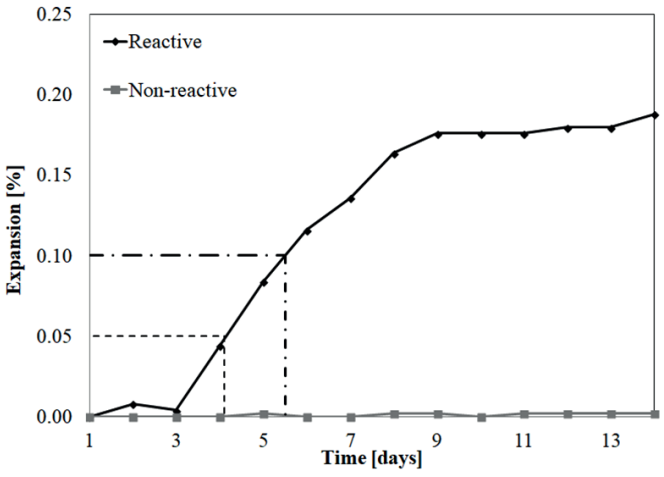

Fig. 1. Length change in mortar bars with reactive and non-reactive aggregate

Expansion of mortars reached 0.05% already after 4 days, and stood at 0.1% after 5 days. Therefore, the aggregate subject to analysis reacted very quickly.

During the same period, white exudations characteristic for ASR were observed on the surface of the bars with opal aggregate, but no cracks were recorded. The surface of mortars made of non-reactive aggregate remained unchanged throughout the testing period.

3.2. Acoustic reactivity response. Analysis of signal parameters, so-called descriptors, constitutes an important aspect of assessment of the progress of corrosion processes using the acoustic emission method. The way material cracking occurs affects the characteristics of acoustic emission signals, i.e. the number of signals, signal duration, rise time, amplitude, signal energy and frequency. Analysis of acoustic activity parameters can be useful in determining the advancement of corrosion processes and examining the corrosion mechanism itself.

The effectiveness of acoustic emission tests depends to a large extent on the procedures for digital processing of signals performed in order to reduce background noise [48]. In order to limit the recording of so-called noise, suitable background noise filters were used: HDT (hit definition time), determining the time between the end of one signal and beginning of another one, HLT (hit lockout time), which prevented measurement of reflected signals, and PDT (peak definition time), set at, respectively, 800 μs, 1000 μs and 200 μs. The specified 40-dB noise threshold for all sensors enabled the elimination of background signals, e.g. operation of the chamber.

During measurements of the acoustic activity of specimens, particularly small-sized specimens, the main source of interference are waves reflected by specimen edges. High-pass and low-pass frequency filters were used to filter them off and record signals with a frequency of 1 kHz to 200 kHz. The main properties of AE signals, i.e. the number of counts, signal strength, amplitude and average frequency as averaged results of measurements from three mortar specimens, were extracted and depicted in Figures 2–5.

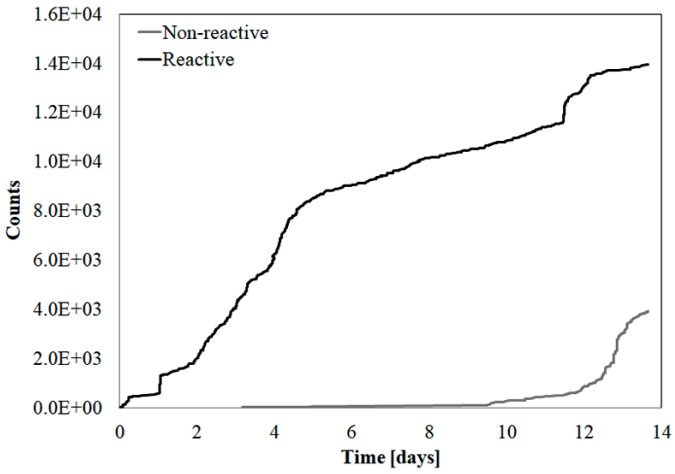

Fig. 2. Cumulative curve of the number of counts in the mortars during 14 days of the experiment

3.2.1. Counts. The number of acoustic emission counts, i.e. the number of detected signals exceeding a specific voltage level, is significantly different in mortars with reactive and non-reactive aggregate (Fig. 2). In the case of reactive aggregate, acoustic activity increases during the first 5 days of reaction and then slows down, after which, on the 12th day, it begins to increase again. The initially significant increase of the number of counts is caused by the quick progress of corrosion processes, which is confirmed by the expansion of the mortars. The increase of the number of counts in the later period is indicative of the growth of microcracks [49].

Mortars made of non-reactive aggregate do not demonstrate any activity in the first 3 days of the experiment. In subsequent days, acoustic activity increased significantly, reaching approx. 400, i.e. approx. 3.5 times less than in the mortars with reactive aggregate.

3.2.2. Signal strength and cumulative signal strength. Figure 3a, 3b shows a point and cumulative chart of AE signal strength for the analyzed mortars with reactive and non-re-

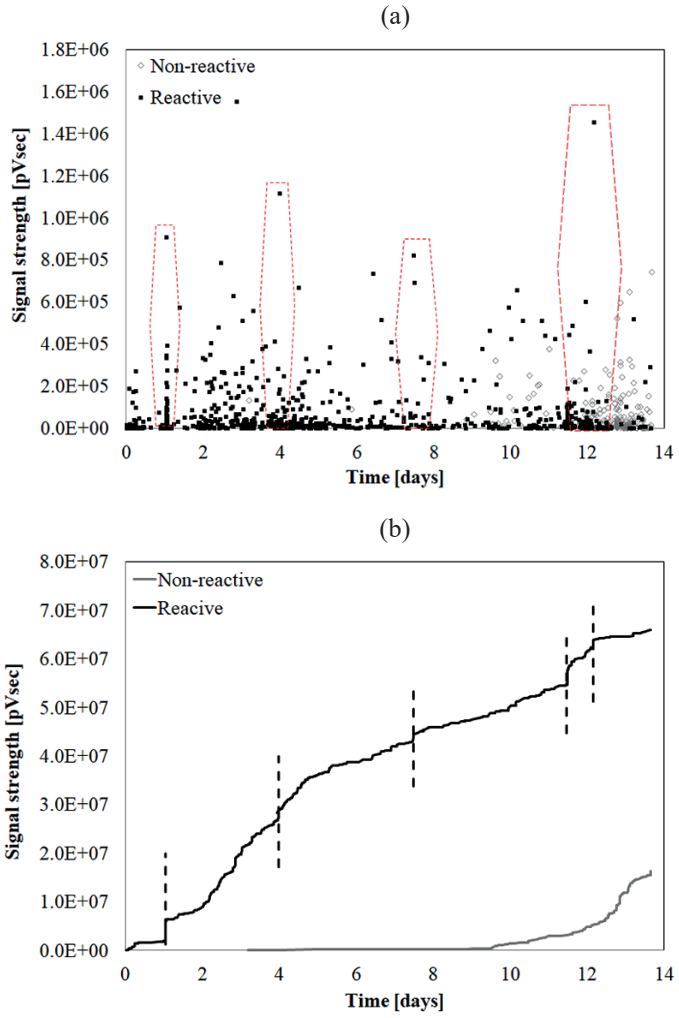

Fig. 3. Variations of AE activity parameters of the specimens during the first 14 days of the experiment (a) AE signal strength, (b) cumulative AE signal strength

active aggregate. Signal strength is one of the AE parameters defined as the area limited by the signal envelope, measured in pVs units. Since it is a measure of energy emitted by the specimen, it may be regarded as an indicator of damage. The increase of signal strength (SS) may be indicative of crack nucleation caused by the creation and accumulation of corrosion products [50].

The produced cumulative curve of signal strength (SS) increases over the entire analyzed period. The shape of the cumulative curve of signal strength (CSS) recorded over time can also be used to draw conclusions about the progress of corrosion processes. Sudden increases of CSS are indicative of damage caused by expansion due to swelling of corrosion products [51].

In the analyzed mortars, the characteristic "elbow" (vertical increase) was observed after the first, fourth and seventh day of the experiment and on the 12–13th days of the test, which was marked in Fig. 3a and 3b with dashed lines. It should be noted that the cumulative curve of signal strength does not flatten out in the analyzed period, which is indicative of continuity of the corrosion processes.

Mortars with non-reactive aggregate demonstrate low acoustic activity and small signal strength until the 9th day of the test. In subsequent days, however, the AE parameter being analyzed begins to rise in an exponentially stable fashion. This may be caused by the formation of small cracks in the mortars due to their storage conditions, i.e. high temperature and relative humidity, or changes in the microstructure occurring during cement hydration.

3.2.3. Amplitude. High levels of acoustic emission signal amplitude depicted in Fig. 4 confirm the high corrosive potential of opal aggregate recorded throughout the experiment. Both individual signals with high amplitudes and sequences of signals with lower amplitudes were recorded in mortars with reactive aggregate. As indicated by Farnam, material cracks

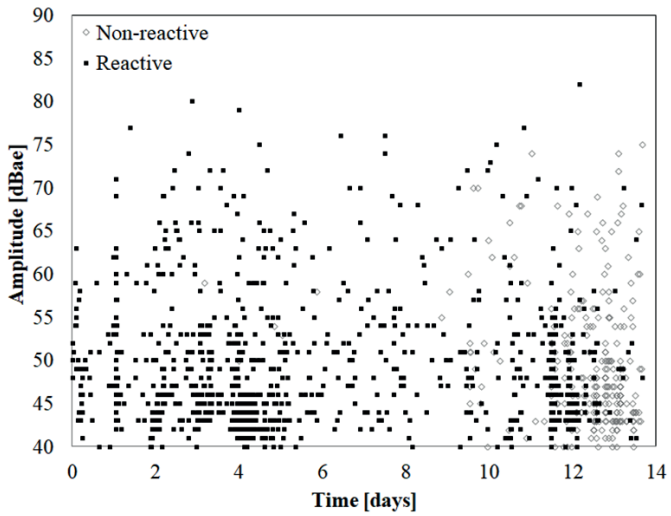

Fig. 4. Distribution of AE amplitude of the specimens during the first 14 days of the experiment

caused by ASR may be gradual or may manifest themselves in the form of a considerable number of cracks over a short period [52]. A significant increase in the amplitude of signals in the mortars made of non-reactive aggregate occurred between the 9th and 14th day.

3.2.4. Average frequency. Important parameters that may provide information about the source of acoustic emission include *inter alia* the average frequency of the AE signal (Fig. 5). The average frequency of the signal is determined for the entire single AE signal, in the form of the ratio of the number of counts to signal duration.

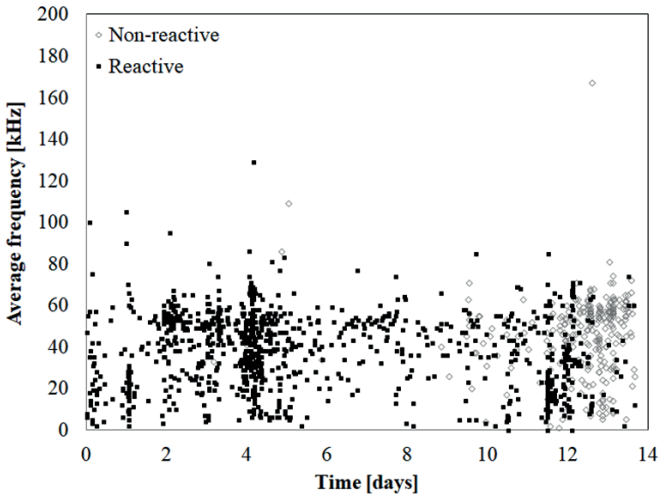

Fig. 5. Point chart of average frequency over time in the mortars on the 14th day of the experiment

The analyzed mortars generate AE signals in a broad frequency range. As indicated by the references, cracks in reactive aggregate are characterized by signals with frequencies higher than those of cracks in the cement paste [52]. The reference value of the signal corresponds to the frequency of 110 kHz. For reactive aggregate, the average frequency is within the range of 0–110 kHz; and in mortars with non-reactive aggregate, the average frequency range is similar.

3.2.5. RA value. The relationship between the RA index, which is a product of signal rise time and amplitude, and the average frequency can be used to classify the measured signals. Cracks can be classified into shear and tensile cracks; high frequency acoustic signals with low RA indices can indicate tensile cracking, and AE signals with low frequency and high RA can most likely be considered shear cracking [53]. As demonstrated in the literature on cracking due to ASR, tensile cracking is most likely to occur in reactive particles while shear cracking is most likely to be observed in the cement matrix [54, 55]. The combination of tensile and shear cracking indicates cracks in the aggregate, cement matrix and ITZ [52]. Parameters RA and AF help separate tensile cracking from shear cracking with a curve

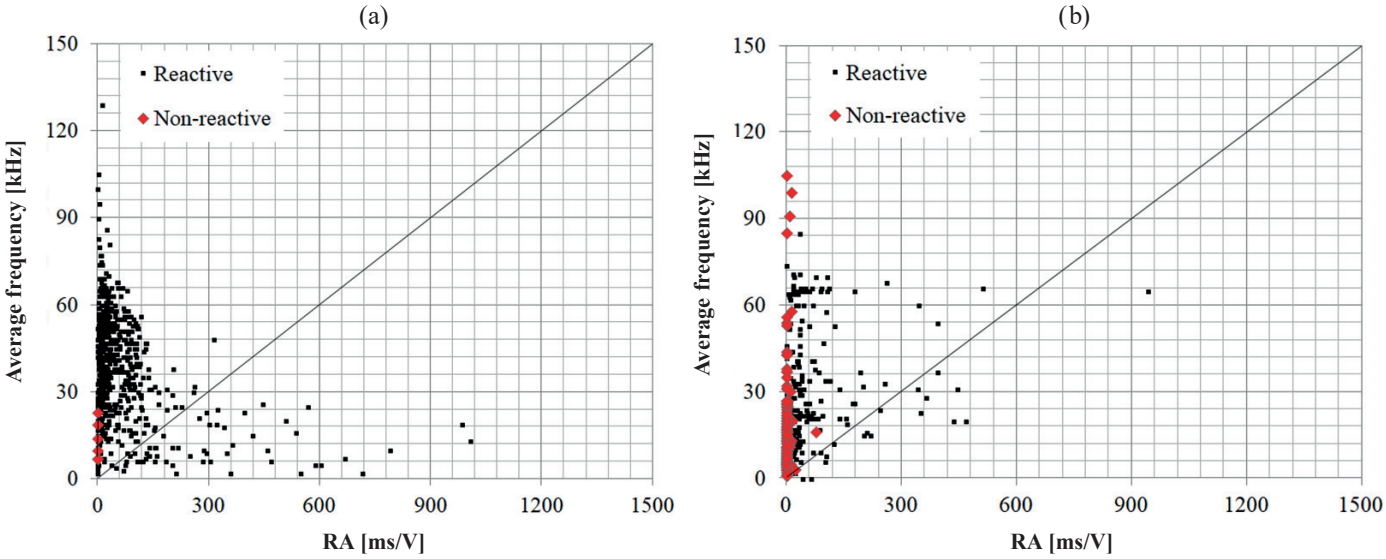

Fig. 6. Variations in RA values and average frequency of samples with and without reactive aggregate during: (a)1–8 days, (b) 9–14 days

at an appropriate slope. The slope of the curve separating the two areas is assumed to be 0.1 Hz*s/V. AE events with an AF to RA ratio greater than 0.1 Hz*s/V can be considered acoustic activity induced by tensile cracking, whereas an AF to RA ratio lower than 0.1 Hz*s/V indicates acoustic activity induced by shear cracking.

In the period being considered until the 9th day, during which the most significant mortar expansion can be recorded, most AE events are located in the left half of the chart, indicating the formation of cracks due to the action of normal forces (Fig. 6a). Signals with parameters that can be considered shear cracking were recorded as well. In accordance with the presented mechanism of concrete damage caused by ASR, microcracks form in the initial stages of reaction in reactive aggregate and at the interface between paste and aggregate due to the formation of reaction products.

The products generate pressure that exceeds the tensile strength of the material. During later stages of the reaction, cracks form in the cement matrix surrounding the reactive aggregate. Between days 9 and 14, in the period of stabilization of the expansion of mortars with reactive aggregate, fewer signals were recorded, indicating primarily cracking, which may be most likely the tensile cracking (Fig. 6b).

In the case of mortars with non-reactive aggregate, signals characterized by low RA and high frequency were recorded after 9 days. These signals, indicating the development of cracks primarily in the aggregate and in the interface area, were caused likely by the specimen storage conditions or cement hydration processes; however, further analyses are necessary to correctly determine the source of the cracks.

3.3. Mortar microstructure. Cracks of opal aggregate, caused by the formation of strongly swelling ASR gel, were primarily observed in the analyzed specimens of mortars with reactive aggregate. Cracks were recorded in the ASR gel itself both on the surface and inside the aggregate, most likely due to drying. In later stages of the reaction, the gel filled the small pores in the cement paste (Fig. 7a–d).

In mortar specimens with reactive aggregate, cracks on the surface of the reactive aggregate and alkali gels forming inside

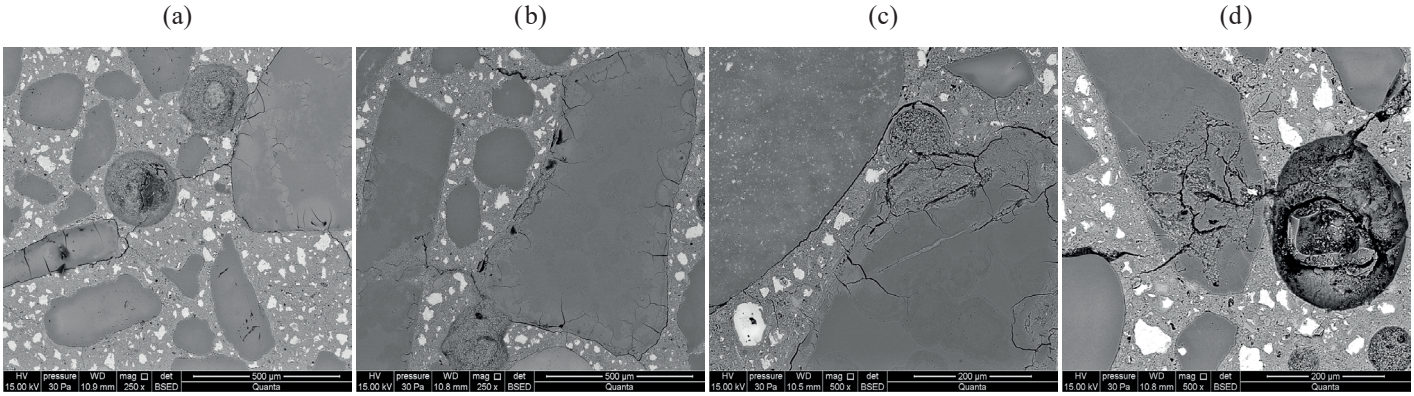

Fig. 7. Microstructure of mortars with reactive aggregate during: 1 day (a), 3 days (b), 7 days (c), 14 days (d)

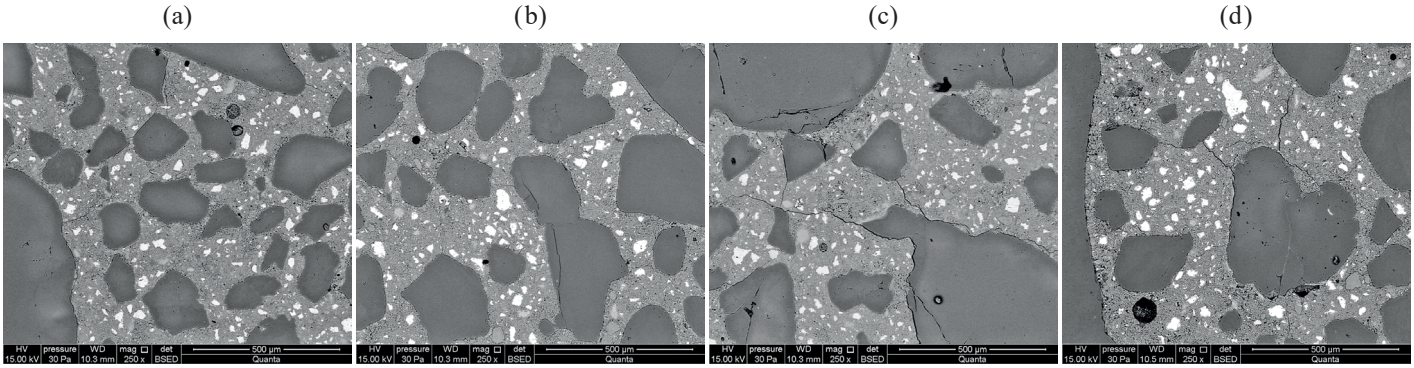

Fig. 8. Microstructure of mortars without reactive aggregate during: 1 day (a), 3 days (b), 7 days (c), 14 days (d)

were observed already after the 1st day of reaction (Fig. 7a). Cracks of reaction products inside the aggregate are indicative of strong hydration of the gels. At the initial stage of the reaction, alkali gels most likely do not generate high expansion pressure, as indicated by the small number of cracks in the cement paste around the reactive aggregate. Significant progress of corrosion processes was recorded in the specimens with opal aggregate after 3 days of reaction (Fig. 7b). Reactive aggregate continued to dissolve further. Large amounts of reaction products with visible voids were formed at the interface between paste and aggregate. The gels that form swell up to a greater extent than the ones observed on the first day, as indicated by the larger cracks of the cement paste around the aggregate. With the progress of the reaction of the aggregate with alkali, the thickness of the gel layer around the aggregate increases, intensifying the cracks around the aggregate itself and the surrounding matrix. The gel also fills the cracks in the aggregate (Fig. 7c).

Microstructural images of mortars with opal aggregate after 14 days of reaction indicate significant advancement of corrosion processes. Crystalline products appear in a part of the area of reactive aggregate, and porosity of the aggregate increases due to the continued dissolution of reactive silica. The extent of cracks in the aggregate itself, at the interface between paste and aggregate and in the cement paste intensifies. Reaction products were sporadically observed in the pores (Fig. 7d).

A small number of silica aggregate cracks and a small amount of cement paste were recorded in the microstructure of mortars with non-reactive aggregate (Fig. 8a–d). The advancement of these changes increased during the later period, after 7 and 14 days. The cracks may be induced by stresses in the material caused by specimen storage conditions and by the existence of aggregate with a weakened structure. This issue requires further analyses.

4. Discussion

The study presented the results of tests conducted in order to determine suitability of the acoustic emission method for the analysis of the progress of corrosion processes, i.e. the so-called internal concrete corrosion. Measurements of the linear elongation of specimens and observations of the microstructure under a scanning electron microscope were conducted at the same time.

The results of the tests indicate that the acoustic emission method is suitable for detection of cracks caused by aggregate reactivity. Due to its high sensitivity, the NDT method applied may be a valuable tool for early detection of alkali corrosion in concrete. The acoustic activity of the analyzed specimens of mortars with reactive aggregate was recorded already on the first day of the test. However, as indicated by the measurements of specimen elongation, determination of potential reactivity of the aggregate with alkali requires a certain advancement of corrosion processes. It should be noted that the formation of microcracks and alkali-aggregate reaction products is reflected by the high acoustic activity of the specimens. The signals have different characteristics because the AE signals are generated by different sources such as: aggregate, matrix and interfacial transition zone. The cracks caused by the alkali-aggregate reaction form in the reactive aggregate, at the interface between paste and aggregate, in the cement matrix and in the ASR gel.

The acoustic activity of mortars with reactive aggregate is well-correlated with the linear elongation of the specimens. The rising signal strength, illustrated in the chart of the cumulative curve of signal strength, proves that the corrosion processes are continuous. As indicated by the analysis of frequency and RA, in the period until the 9th day of reaction, the developing microcracks are caused primarily by normal stresses, which is indicative of corrosion taking place primarily in the reactive aggregate. In turn, the cracks at the interface between paste and aggregate can be classified as shear cracking. Stabilization of expansion at a later stage of the experiment does not result in the impediment of acoustic activity in the mortars with reactive aggregate.

Mortars with non-reactive aggregate demonstrated low acoustic activity. The signals recorded, particularly the very few signals recorded until the 9th day of the test, were characterized by low amplitude and signal strength but different average frequency. Beginning with day 10, in turn, acoustic activity was characterized by different descriptors. The amplitude and signal strength increased and the recorded events had different frequency, too. However, in the microstructure of mortars,

especially after 7 days of storage, some cracks in aggregates and cement paste were observed. This issue requires further analyses. Furthermore, when analyzing the behavior of non-reactive aggregate in a 1M NaOH solution and temperature of 80°C, Rashid et al. pointed to the increase in mortar expansion after several days. When analyzing the relation between the expansion and cumulative average non-linearity parameters in the NIRAS (non-linear impact resonance acoustic spectroscopy) method, they revealed a weak correlation. However, it was emphasized that in the case of mortars with reactive aggregate, there is a strong interdependency between mortar expansion, the DRI (damage index rating) and cumulative average non-linearity parameters [56].

The tests conducted by the authors indicate that the analyzed opal aggregate reacts both through silica dissolution and solid-state reaction, as indicated in the works of Scrivener et al. [57, 58]. Cracks caused by the formation of strongly hydrated alkali gels were observed on the first day of the test on the aggregate surface and inside the aggregate. An increase of aggregate porosity, caused by silica dissolution, was also observed on subsequent days. Different advancements of corrosion processes, including microcracks, were recorded depending on aggregate size. Also, smaller aggregate corroded more quickly, as confirmed by examinations of microstructure carried out after the first day of the test. The progress of corrosion processes was accompanied by an increase in the volume of reaction products, concentrated in the reactive aggregate and at the interface between paste and aggregate.

A comparison of the results of mortar specimen elongation tests with the results of acoustic emission analyses demonstrated a significant consistency. Opal aggregate is highly reactive, and its reaction with alkali is quick. High acoustic activity of mortars with opal aggregate was recorded already on the first day of the test. This proves the high sensitivity and suitability of the acoustic emission method for testing of corrosion processes. Thorough analysis of AE descriptors, in turn, makes it possible to describe the mechanism of material damage.

5. Conclusions

The paper demonstrates that the AE method allows for detecting cracks in mortars with reactive aggregate. Energy parameters, i.e. signal strength, counts and amplitude, can all be used for indicating cracks nucleation and RA while the average frequency relationship can serve to determine which of the mortar components is subject to cracking. This can help in monitoring the course of reaction and determining the degree of corrosion processes. The following conclusions can be formulated based on these results:

- Due to the anisotropic structure of mortar, the evaluation based solely on frequency parameters can be erroneous to a large extent. The proposed approach facilitates the monitoring of the occurring processes and provides the basis for proposing the SHM tool as a means of monitoring the impact of aggregate reactivity on the structure's durability.
- Application of the energy parameters analysis allows for determining the source of the cracks, i.e. matrix, aggregate cracking as well as aggregate and interfacial transition zones. The proposed analytic approach which uses energy parameters allows for monitoring the destructive processes' intensity.
- The authors have confirmed the acoustic emission method's high sensitivity in the analysis of the grout damage degree due to aggregate reaction with alkali. The results of the obtained analyses confirm the microscopic observations, indicating substantial progress of corrosion processes in the grouts with opal aggregate and a minor quantity of cracks in the grouts with non-reactive aggregate.
- Cracking caused by aggregate reaction with alkali was detected earlier when applying the acoustic emission method than in the traditional approach of measuring the samples' linear changes. This can be helpful in determining the kinetics of the occurring corrosion processes and their early detection.

References

[1] PN-EN 206+A1:2016–12 Concrete – Specification, performance, production and conformity.

[2] T. Ahmed, E. Burley, S. Rigden, and A.I. Abu-Tair, "The effect of alkali reactivity on the mechanical properties of concrete", *Constr. Build. Mat*. 17, 123–144 (2003)

[3] Y. Zhou, H. Tian, L. Sui, F. Xing, and N. Han, "Strength Deterioration of Concrete in Sulfate Environment: An Experimental Study and Theoretical Modeling", *Adv. Mater. Sci. Eng.* (2015).

[4] E. Mohseni, W. Tang, and H. Cui, "Chloride Diffusion and Acid Resistance of Concrete Containing Zeolite and Tuff as Partial Replacements of Cement and Sand", *Mater.* 10, (2017).

[5] Alkali-Silica Reaction Mechanisms and Detection: An Advanced Understanding, *Publication No. FHWA-HRT-14–079*, 2014.

[6] M.S. Islam and S.A. Akhtar, "Critical Assessment to the Performance of Alkali-Silica Reaction (ASR) in Concrete", *Can. Chem. Trans.* 1(4), 253–266 (2013).

[7] G.M. Ahlstrom, "The United States Federal Highway Administration's alkali–silica reactivity development and deployment program", *Proc. 14th International Conference on Alkali Aggregate Reactions*, Austin, TX, 2012.

[8] M.D.A. Thomas, B. Fournier, and K.J. Folliard, "Report on determining the reactivity of concrete aggregates and selecting appropriate measures for preventing deleterious expansion in new concrete construction", *Publication No. FHWA-HIF-09–001*, 2008.

[9] Z. Owsiak, J. Zapała-Sławeta, and P. Czapik, "Sources of the Gravel Aggregate Reaction with Alkalis in Concrete", *Cem Lime Concr.* 17 (3), 149–153 (2012).

[10] J. Zapała-Sławeta and Z. Owsiak, " The role of lithium compounds in mitigating alkali-aggregate reaction", *Constr. Build. Mater.* 115, 299–303 (2016).

[11] Z. Owsiak and J. Zapala-Slaweta, "The lithium nitrate effect on the concrete expansion caused by alkali-silica reaction in concrete of gravel aggregate", *Cem. Lime Concr.* 20(1), 25–31 (2015).

[12] Z. Owsiak and J. Zapała-Sławeta, "The course of the alkali-aggregate reaction in the presence of lithium nitrate", *Ceram – Silik.* 57(2), 138–145 (2013).

[13] Z. Owsiak, J. Zapała-Sławeta, and P. Czapik, "Diagnosis of concrete structures distress due to alkali-aggregate reaction", *Bull. Pol. Ac.: Tech.* 63(1), 23–29 (2015).
[14] A.B. Poole, "Introduction to alkali–aggregate reaction in concrete", R.N. Swamy (Ed.), *The Alkali Silica Reaction in Concrete*, Van Nostrand Reinhold, New York, 1992.
[15] H. Wang and J.E. Gillot, "Mechanism of alkali–silica reaction and significance of calcium hydroxide", *Cem. Concr. Res.* 21, 647–654 (1991).
[16] F. Rajabipour, E. Giannini, C. Dunant, J.H. Ideker, and M.D.A. Thomas, "Alkali–silica reaction: Current understanding of the reactionmechanisms and the knowledge gaps", *Cem. Concr. Res.* 76,130–146 (2015).
[17] Z. Owsiak, The alkali-silica reaction in concrete. *Pol. Cer. Bull.: Ceramics* 72, CD-ROM (2002), [in Polish].
[18] J. Zapała-Sławeta and Z. Owsiak, "Influence of exposure conditions on the efficacy of lithium nitrate in mitigating alkali silica reaction", *IOP Conference Series-Materials Science and Engineering*, p.245, 2017.
[19] J. Zapała-Sławeta and Z.Owsiak, "Effect of lithium nitrate on the reaction between opal aggregate and sodium and potassium hydroxides in concrete over a long period of time", *Bull. Pol. Ac.: Tech.* 65(6), 773–778 (2017).
[20] M. Sargolzahi, S.A. Kodjo, P. Rivard, and J. Rhazi, "Effectiveness of nondestructive testing for the evaluation of alkali–silica reaction in concrete" *Constr. Build. Mater*. 24, 1398–1403 (2010).
[21] P. Rivard and F. Saint-Pierre, "Assessing alkali-silica reaction damage to concrete with non-destructive methods: From the lab to the field",. *Constr. Build. Mater.* 23, 902–909 (2009).
[22] C. Bernstone, H. Sundblom, P.O. Bjorkqvist, G. Gudmudsson, O. Klinghofer, I. Markey et al., "Non-destructive testing of concrete structure – an owner guide", unpublished documents from the non-destructive testing for integrity determination of concrete structure, 2004.
[23] F. Saint-Pierre, "Monitoring of ASR evolution with ultrasonic method and seismic tomography", (in French) Ph.D. Thesis, Department of Civil Engineering, Université de Sherbrooke, 2006.
[24] G. Świt, A. Krampikowska, and M.Ch. Luong, "A prototype system for acoustic emission-based structural health monitoring of My Thuan bridge", *Proceedings of 2016 Prognostics and System Health Management Conference (PHM-Chengdu)*, 624–630 (2016).
[25] P. Olaszek, J.R. Casas, and G. Swit, "On-site assessment of bridges supported by acoustic emission", *Proceedings of the Institution of Civil Engineers-Bridge Engineering*, 169(2), 81–92 (2016).
[26] G. Świt, "Acoustic Emission Method for Locating and Identifying Active Destructive Processes in Operating Facilities", *Appl. Sci. (Basel)*, (2018).
[27] Y. Kawasaki, T. Wakuda, T. Kobarai, and M. Ohtsu, "Corrosion mechanisms in reinforced concrete by acoustic emission", *Constr. Build. Mater.* 48, 1240–1247 (2013).
[28] S. Patil, B. Karkare, and S. Goyal, "Acoustic emission vis-ŕ-vis electrochemical techniques for corrosion monitoring of reinforced concrete element", *Constr. Build. Mater.* 68, 326–332 (2014).
[29] A. Zaki, H.K. Chai, D.G. Aggelis, and N. Alver, "Non-destructive evaluation for corrosion monitoring in concrete: A review and capability of acoustic emission technique", *Sensors,* 15 (2015).
[30] Z. Ranachowski, "Acoustic emission in diagnostics of civil engineering structures", Roads and Bridges, 2012.
[31] G. Świt and A. Krampikowska, "Influence of the number of acoustic emission descriptors on the accuracy of destructive process identification in concrete structures", *Proceedings of 2016 Prognostics and System Health Management Conference (PHM-Chengdu)*, 624–630 (2016).
[32] ASTM E 650: Standard Guide for Mounting Piezoelectric Acoustic Emission Transducers, ASTM International, West Conshohocken, 2002.
[33] P. Olaszek, G. Swit, and J.R. Casas, "Proof load testing supported by acoustic emission. An example of application", *Proc. 5th International Conference on Bridge Maintenance, Safety and Management and Life-Cycle Organization (IABMAS)*, Philadelphia, 688–694 (2010).
[34] G. Świt, "Evaluation of compliance changes in concrete beams reinforced by glass fiber reinforced plastics using acoustic emission" *J. Mater. Civil Eng.* 16(5), 414–418 (2004).
[35] F. Weise, K. Voland, S. Pirskawetz, and D. Meinel, "Innovative measurement techniques for characterising internal damage processes in concrete due to ASR", *Proc. 14th International Conference on Alkali-Aggregate Reaction (ICAAR)*, Austin (Texas), 2012.
[36] M. Abdelrahman, M.K. ElBatanouny, P. Ziehl, J. Fasl, C.J. Larosche, and J. Fraczek, "Classification of alkali–silica reaction damage using acoustic emission: A proof-of-concept study", *Constr. Build. Mater.* 95, 406–413 (2015).
[37] T. Lokajíček, R. Přikryl, S. Šachlová, and A. Kuchařová, "Acoustic emission monitoring of crack formation during alkali silica reactivity accelerated mortar bar test", *Eng. Geol.* 220, 175–182 (2017).
[38] M. Pour-Ghaz, R. Spragg, J. Castro, and J. Weiss, "Can acoustic emission be used to detect alkali silica reaction earlier than length change tests?", *Proc. 14th International Conference on Alkali Aggregate Reaction in Concrete*, Austin, TX, 2012.
[39] M. Bacharz, B. Goszczyńska, and W. Trąmpczyński, "Analysis of destructive processes in unloaded early age concrete with acoustic emission method", *Procedia Eng.* 108, 245–253 (2015).
[40] K. Ono, "Application of acoustic emission for structure diagnosis", in *Diagnostics Struct Heal Monit*; 2(58), 3–18 (2011).
[41] M. Ohtsu, T. Isoda, and Y.Tomoda, "Acoustic emission techniques standardized for concrete structures", *J. Acoustic Emission*, 25 (2007).
[42] JCMS-IIIB5706. *Monitoring Method for Active Cracks in Concrete by Acoustic Emission*; Federation of Construction Material Industries: Tokyo, Japan, pp. 23–28, 2003.
[43] J. Zapała-Sławeta and G. Świt, "Monitoring of the impact of lithium nitrate on the alkali-aggregate reaction using acoustic emission methods", *Materials*, 12(1), 20(2019).
[44] J. Zapała-Sławeta, "The effect of meta-halloysite on alkali-aggregate reaction in concrete", *Mater. Struct.* 50(5), 2017.
[45] ASTM C 227 – 10 Standard Test Method for Potential Alkali Reactivity of Cement- Aggregate Combinations (Mortar-Bar Method).
[46] L.Gołaski, B.Goszczyńska, G.Świt, and W.Trąmpczyński, "System for the global monitoring and evaluation of damage processes developing within concrete structures under service load", *Balt. J. Road Bridge Eng.* 7(4), 237- 245 (2012).
[47] B. Goszczyńska, G. Świt, and W. Trąmpczyński, "Monitoring of Active Destructive Processes as a Diagnostic Tool for the Structure Technical State Evaluation", *Bull. Pol. Ac.: Tech.* 61(1), 97–108 (2013).

[48] L. Hasse, L. Spiralski, and J. Šikula, "Measurement and processing of acoustic emission signals in diagnostics of structures" *The Scientific Papers of Faculty of Electrical and Control Engineering Gdańsk University of Technology*, 20, 77–84 (2004), [in Polish].

[49] P.J. Prem and A.R. Murthy, "Acoustic emission monitoring of reinforced concrete beams subjected to four-point-bending", *Appl. Acoust.* 117, 28–38 (2017).

[50] W. Vélez, F. Matta, and P. Ziehl, "Acoustic emission intensity analysis of corrosion in prestressed concrete piles", *AIP Conference Proceedings,* 1581, pp. 888, 2014.

[51] M. Benedetti, G. Loreto, F. Matta, and A. Nanni, "Acoustic emission monitoring of reinforced concrete under accelerated corrosion", *J. Mater. Civ. Eng.* 25(8),1022–9 (2013).

[52] Y. Farnam, M.R. Geiker, D. Bentz, and J. Weiss, "Acoustic emission waveform characterization of crack origin and mode in fractured and ASR damaged concrete", *Cement Concrete Comp.* 60, 135–145 (2015).

[53] K. Ohno and M. Ohtsu, "Crack classification in concrete based on acoustic emission", *Constr Build Mater.* 24, 2339–46 (2010).

[54] S Chatterji, N Thaulow, and AD Jensen, "Studies of alkali–silica reaction. Part 5. Verification of a newly proposed reaction mechanism", *Cem Concr Res.* 19, 177–83 (1989).

[55] S. Chatterji, N. Thaulow, and A.D. Jensen, Studies of alkali–silica reaction, part 6. Practical implications of a proposed reaction mechanism", *Cem Concr Res.* 18, 363–6 (1989).

[56] M. Rashidi, M.C. Knapp, A. Hashemi, J-Y Kim, K. Donnell, R. Zoughi, L.J. Jacobs, and K.E. Kurtis, "Detecting alkali-silica reaction: A multi-physics approach", *Cement Concrete Comp.* 73, 123–135 (2016).

[57] K.L. Scrivener and P.J.M. Monteiro, "The alkali silica recation in monolithic opal", *J. Am. Ceram. Soc.* 77 (11), 2849–56 (1994).

[58] S.V. Liang, K.L. Scrivener, and P.L. Pratt, "An investigation of alkali-silica reaction in seven-year old and model concretes using S.E.M. end E.D.S", *Proc. 9th International Conference on Alkali-Aggregate Reaction*, London 1992, pp.579–586.